Trinuclear Zn(II) and Cu(II) Homo and Heterotrimetallic Complexes Involving D-Glucopyranosyl and Biscarboxylate Bridging Ligands. A Substrate Binding Model of Xylose Isomerases

Tomoaki Tanase,*,† Hiromi Inukai,† Tomoko Onaka,† Merii Kato,† Shigenobu Yano,† and Stephen J. Lippard‡

Department of Chemistry, Faculty of Science, Nara Women's University, Nara-shi, Nara 630-8285, Japan, and Department of Chemistry, Massachusetts Institute of Technology, Cambridge, Massachusetts 02139

Received December 19, 2000

Reactions of $MCl_2 \cdot nH_2O$ with *N*,*N*′-bis(D-glucopyranosyl)-1,4,7-triazacyclononane ((D-Glc)$_2$-tacn), which was formed from D-glucose and 1,4,7-triazacyclononane (tacn) in situ, afforded a series of mononuclear divalent metal complexes with two β-D-glucopyranosyl moieties, [M{(D-Glc)$_2$-tacn}Cl]Cl (M = Zn (**11**), Cu (**12**), Ni (**13**), Co (**14**)). Complexes **11**−**14** were characterized by analytical and spectroscopic measurements and X-ray crystallography and were found to have a distorted octahedral M(II) center ligated by the pentacoordinate *N*-glycoside ligand, (β-D-glucopyranosyl)$_2$-tacn, and a chloride anion. Each D-glucose moiety is tethered to the metal center through the β-*N*-glycosidic bond with tacn and additionally coordinated via the C-2 hydroxyl group, resulting in a λ-gauche five-membered chelate ring. When L-rhamnose (6-deoxy-L-mannose) was used instead of D-glucose, the nickel(II) complex with two β-L-rhamnopyranosyl moieties, [Ni{(D-Man)$_2$-tacn}(MeOH)]Cl$_2$ (**15**), was obtained and characterized by an X-ray analysis. Reactions of **11** (M = Zn) with [Zn(XDK)(H$_2$O)] (**21**) or [Cu(XDK)(py)$_2$] (**22**) (H$_2$XDK = *m*-xylylenediamine bis(Kemp's triacid imide)) yielded homo and heterotrimetallic complexes formulated as [Zn$_2$M′{(D-Glc)$_2$-tacn}$_2$(XDK)]Cl$_2$ (M′ = Zn (**31**), Cu (**32**)). The similar reactions of **12** (M = Cu) with complex **21** or **22** afforded [Cu$_2$M′{(D-Glc)$_2$-tacn}$_2$(XDK)]Cl$_2$ (M′ = Cu (**33**), Zn (**34**)). An X-ray crystallographic study revealed that complexes **31** and **34** have either $Zn^{II}{}_3$ or $Cu^{II}Zn^{II}Cu^{II}$ trimetallic centers bridged by two carboxylate groups of XDK and two D-glucopyranosyl residues. The M···M′ separations are 3.418(3)−3.462(3) Å (**31**) and 3.414(1)−3.460(1) Å (**34**), and the M···M′···M angles are 155.18(8)° (**31**) and 161.56(6)° (**34**). The terminal metal ions are octahedrally coordinated by the (D-Glc)$_2$-tacn ligand through three nitrogen atoms of tacn, two oxygen atoms of the C-2 hydroxyl groups of the carbohydrates, and a carboxylate oxygen atom of XDK ligand. The central metal ions sit in a distorted octahedral environment ligated by four oxygen atoms of the carbohydrate residues in the (D-Glc)$_2$-tacn ligands and two carboxylate oxygen atoms of XDK. The deprotonated β-D-glucopyranosyl unit at the C-2 hydroxyl group bridges the terminal and central ions with the C-2 μ-alkoxo group, with the C-1 *N*-glycosidic amino and the C-3 hydroxyl groups coordinating to each metal center. Complexes **31**−**34** are the first examples of metal complexes in which D-glucose units act as bridging ligands. These structures could be very useful substrate binding models of xylose or glucose isomerases, which promote D-glucose D-fructose isomerization by using divalent dimetallic centers bridged by a glutamate residue.

Introduction

Elucidation of interactions between carbohydrates and metal ions is of importance in bioinorganic chemistry, since many sugar-metabolizing enzymes and some sugar-binding proteins function with a variety of divalent metal ions, such as Mg^{2+}, Mn^{2+}, Co^{2+}, Zn^{2+}, and Ca^{2+}.[1,2] In some cases, carboxylate-bridged divalent dimetallic centers, a ubiquitous motif in many hydrolytic metalloenzymes,[3] also play important roles via interactions with carbohydrates. Xylose (glucose) isomerases promote the aldose−ketose isomerization by utilizing glutamate-bridged dimetallic centers of Mg^{2+}, Mn^{2+}, or Co^{2+} ions in the active sites (Figure 1a). The substrate (D-xylose or D-glucose) in the open-chain form directly interacts with both metal ions. Formation of a bridging C-2 hydroxyl group is proposed to be crucial for the 1,2-hydride shift of the carbohydrate, as depicted in Figure 1b.[2]

* To whom correspondence should be addressed. Fax: +81 742−20−3399. E-mail: tanase@cc.nara-wu.ac.jp.

† Nara Women's University.

‡ Massachusetts Institute of Technology.

(1) (a) Kennedy, J. F.; White, C. A. *Bioactive Carbohydrates in Chemistry, Biochemistry and Biology*; John Wiley & Sons: New York, 1983. (b) Zhang, Y.; Liang, J.-Y.; Huang, S.; Ke, H.; Lipscomb, W. N. *Biochemistry* **1993**, *32*, 17. (c) Xue, Y.; Huang, S.; Liang, J.-Y.; Zhang, Y.; Lipscomb, W. N. *Proc. Natl. Acad. Sci. U.S.A.* **1994**, *91*, 12482. (d) Hardman, K. D.; Agarwal, R. C.; Freiser, M. *J. Mol. Biol.* **1982**, *157*, 69. (e) Weis, W. I.; Kahn, R.; Fourme, R.; Drickamer, K.; Hendrickson, W. A. *Science* **1991**, *254*, 1608. (f) Weis, W. I.; Drickamer, K.; Hendrickson, W. A. *Science* **1992**, *360*, 127. (g) Ng, K. K.-S.; Weis, W. I. *Biochemistry* **1997**, *36*, 979. (h) Ng, K. K.-S.; Park-Synder, S.; Weis, W. I. *Biochemistry* **1998**, *37*, 17965.

(2) (a) Farber, G. K.; Glasfeld, A.; Tiraby, G.; Ringe, D.; Petsko, G. A. *Biochemistry* **1989**, *28*, 7289. (b) Jenkins, J.; Janin, J.; Rey, F.; Chiadmi, M.; Tilbeurgh, H.; Lasters, I.; Maeyer, M. D.; Belle, D. V.; Wodak, S. J.; Lauwereys, M.; Stanssens, P.; Mrabet, N. T.; Snauwaert, J.; Matthyssens, G.; Lambeir, A.-M. *Biochemistry* **1992**, *31*, 5449. (c) Whitlow, M.; Howard, A. J.; Finzel, B. C.; Poulos, T. L.; Winborne, E.; Gilliland, G. L. *Proteins* **1991**, *9*, 153. (d) Lavie, A.; Allen, K. N.; Petsko, G. A.; Ringe, D. *Biochemistry* **1994**, *33*, 5469.

10.1021/ic001419t CCC: $20.00
Published on Web 06/23/2001

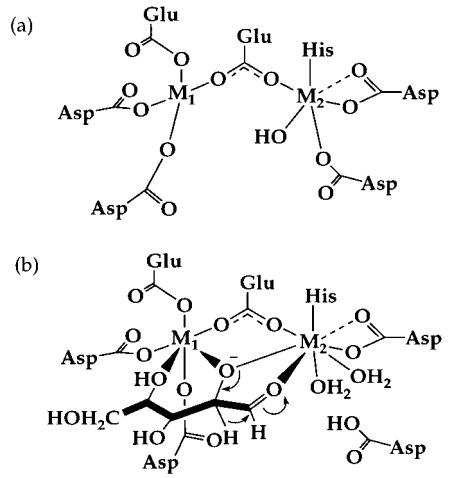

Figure 1. (a) The structures of the active site of xylose isomerase and (b) a proposed structure of the substrate binding and activation (ref 2).

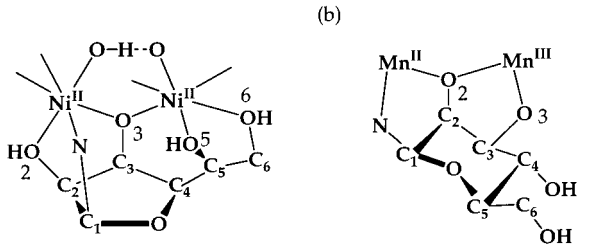

Figure 2. The carbohydrate-bridging structures of (a) $[Ni_2(N,N'$-(D-Man)$_2-N,N'$-Me$_2$en)$(N-$(D-Man)-N,N'-Me$_2$en)$(CH_3OH)]Cl_2$ (**1**) and (b) $[\{Mn^{II}(aldose)_3\text{-tren}\}_2Mn^{III}(H_2O)]^{3+}$ (**4**) (refs 7c and 8b).

We have studied the chemistry of transition-metal complexes with carbohydrates by utilizing an *N*-glycosidic bond to tether sugars onto metals under neutral conditions.[4−7] The behavior and reactivity of aldoses introduced at dimetallic centers is of special interest. Dinuclear and trinuclear transition metal complexes in which mannose-type aldoses (D-mannose and L-rhamnose (6-deoxy-L-mannose)) with a 2,3-cis configuration act as bridging ligands have been obtained (Figure 2). The dinuclear Ni(II) complex, $[Ni_2(N,N'$-(D-Man)$_2$-N,N'-Me$_2$en)$(N-$(D-Man)-N,N'-Me$_2$en)$(CH_3OH)]Cl_2$ (**1**), utilizes a β-D-mannosylamine moiety in its furanose form to join two metals with all-*cis* donors, the C-3 alkoxo group acting as a monoatomic bridge (Figure 2a).[8] C-2 Epimerization of aldoses occurs through stereospecific rearrangement of the sugar carbon skeleton or inversion of a 1,2-carbon fragment, with related nickel(II) complexes.[9] Similar bridged structures of deprotonated D-mannofuranose occur in homoleptic trivalent dimetallic complexes, $Ba_2[M^{III}_2(\beta$-D-mannose$^{5-})_2]$ (**2**) (M = Fe, V, Cr, Al, Ga).[10] An all-*cis*-bridging mode of furanose has also been observed in $[Mo^{VI}_2O_4(\mu$-O)(D-lyxose$^{2-})]$ (**3**),[11] where the C-2 and C-5 hydroxyl groups are doubly deprotonated, both serving as μ-alkoxo bridges. More recently, we have synthesized the $Mn^{II}Mn^{III}Mn^{II}$ trinuclear complexes, $[\{Mn^{II}(aldose)_3\text{-tren}\}_2Mn^{III}(H_2O)]^{3+}$ (**4**)[7c] (aldose = D-Man, L-Rha), by reaction of the heptacoordinate mononuclear Mn(II) complexes of $[Mn^{II}(aldose)_3\text{-tren})\}]^{2+}$ with Mn^{2+} ions. In the trimanganese complexes, a β-mannopyranosyl skeletal unit with a chair conformation bridges the two manganese ions, with the C-2 μ-alkoxo group playing a key function and the C-1 *N*-glycosidic amino and C-3 alkoxo groups coordinating to each metal center (Figure 2b).

In contrast to the mannose-type aldoses, no structurally characterized example of a dimetallic center bridged by D-glucose has been reported thus far, due presumably to the low affinity of metal ions for the thermodynamically stable $^4C_1$ pyranoid form. D-Glucose is the most naturally abundant carbohydrate, and its transformations at dimetallic centers, mimicking biological systems such as xylose isomerases, are important to investigate. We wish to report herein the homo- and heterotrimetallic Zn(II) and Cu(II) complexes, $[M_2M'\{(D\text{-}Glc)_2\text{-tacn}\}_2(XDK)]Cl_2$ (**31**−**34**), prepared by stepwise construction from the D-glucose-binding mononuclear complexes, $[M\{(D\text{-}Glc)_2\text{-tacn}\}Cl]Cl$. We also present mononuclear complexes having the biscarboxylate dinucleating ligand XDK, where tacn is 1,4,7-triazacyclononane and H_2XDK is *m*-xylylenediamine bis(Kemp's triacid imide). The present trinuclear complexes are the first examples in which two metal ions are bridged by a D-glucopyranosyl and a carboxylate group and thus model features of substrate binding in xylose (glucose) isomerases.

Experimental Section

Materials. All reagents were of commercial grade and used as received. *m*-Xylylenediamine bis(Kemp's triacid imide) (H_2XDK),[12] 1,4,7-triazacyclononane (tacn),[13] $Na_2XDK\cdot4H_2O$,[14] and $[Zn(XDK)(H_2O)]$ (**21**)[15] were prepared by known methods. [1-^{13}C]-D-Glucose was purchased from Aldrich. The following abbreviations are used: N,N'-bis(D-glucopyranosyl)-1,4,7-triazacyclononane, $(D\text{-}Glc)_2$-tacn; N,N'-bis-(L-rhamnopyranosyl)-1,4,7-triazacyclononane, $(L\text{-}Rha)_2$-tacn; D-Glc, D-glucose; D-Man, D-mannose; and L-Rha, L-rhamnose (6-deoxy-L-mannose).

Measurements. Electronic absorption spectra were recorded on a Shimadzu UV-3100 spectrometer, and circular dichroism spectra were recorded on Jasco J-720 and -730 spectropolarimeters. IR spectra were measured on KBr pellets with a Jasco FT/IR-410 spectrometer. ^{1}H NMR spectra were measured on a Varian Gemini2000 instrument at 300 MHz.

(3) (a) Karlin, K. D. *Science* **1993**, *261*, 701, and references therein. (b) Vallee, B. L.; Auld, D. S. *Biochemistry* **1993**, *32*, 6493.
(4) (a) Tanase, T.; Nouchi, R.; Doi, M.; Kato, M.; Sato, Y.; Ishida, K.; Kobayashi, K.; Sakurai, T.; Yamamoto, Y.; Yano, S. *Inorg. Chem.* **1996**, *35*, 4848. (b) Tanase, T.; Yasuda, Y.; Onaka, T.; Yano, S. *J. Chem. Soc., Dalton Trans.* **1998**, 345, and references therein.
(5) (a) Tanase, T.; Nakagoshi, M.; Teratani, A.; Kato, M.; Yamamoto, Y.; Yano, S. *Inorg. Chem.* **1994**, *33*, 6. (b) Yano, S.; Nakagoshi, M.; Teratani, A.; Kato, M.; Tanase, T.; Yamamoto, Y.; Uekusa, H.; Ohashi, Y. *Mol. Cryst. Liq. Cryst.* **1996**, *276*, 253. (c) Yano, S.; Nakagoshi, M.; Teratani, A.; Kato, M.; Onaka, T.; Iida, M.; Tanase, T.; Yamamoto, Y.; Uekusa, H.; Ohashi, Y. *Inorg. Chem.* **1997**, *36*, 4187.
(6) (a) Tanase, T.; Onaka, T.; Nakagoshi, M.; Kinoshita, I.; Shibata, K.; Doe, M.; Fujii, J.; Yano, S. *Chem. Commun.* **1997**, 2115. (b) Tanase, T.; Onaka, T.; Nakagoshi, M.; Kinoshita, I.; Shibata, K.; Doe, M.; Fujii, J.; Yano, S. *Inorg. Chem.* **1999**, *38*, 3150.
(7) Yano, S.; Doi, M.; Tamakoshi, S.; Mori, W.; Mikuriya, M.; Ichikawa, A.; Kinoshita, I.; Yamamoto, Y.; Tanase, T. *Chem. Commun.* **1997**, 997. (b) Tanase, T.; Tamakoshi, S.; Doi, M.; Mori, W.; Yano, S. *Inorg. Chim. Acta* **1997**, *266*, 5. (c) Tanase, T.; Tamakoshi, S.; Doi, M.; Mikuriya, M.; Sakurai, H.; Yano, S. *Inorg. Chem.* **2000**, *39*, 692.
(8) (a) Tanase, T.; Kurihara, K.; Yano, S.; Kobayashi, K.; Sakurai, T.; Yoshikawa, S. *J. Chem. Soc., Chem. Commun.* **1985**, 1562. (b) Tanase, T.; Kurihara, K.; Yano, S.; Kobayashi, K.; Sakurai, T.; Yoshikawa, S.; Hidai, M. *Inorg. Chem.* **1987**, *26*, 3134.
(9) (a) Tanase, T.; Shimizu, F.; Yano, S.; Yoshikawa, S. *J. Chem. Soc., Chem. Commun.* **1986**, 1001. (b) Tanase, T.; Shimizu, F.; Kuse, M.; Yano, S.; Yoshikawa, S.; Hidai, M. *J. Chem. Soc., Chem. Commun.* **1987**, 659. (c) Tanase, T.; Shimizu, F.; Kuse, M.; Yano, S.; Yoshikawa, S.; Hidai, M. *Inorg. Chem.* **1988**, *27*, 4085.
(10) Burger, J.; Gack, C.; Klüfers, P. *Angew. Chem., Int. Ed. Engl.* **1995**, *34*, 2647.
(11) Taylor, G. E.; Waters, J. M. *Tetrahedron Lett.* **1981**, *22*, 1277.
(12) Rebek, J., Jr.; Marshall, L.; Wolak, R.; Parris, K.; Killoran, M.; Askew, B.; Nemeth, D.; Islam, N. *J. Am. Chem. Soc.* **1985**, *107*, 7476.
(13) (a) Richman, J. E.; Oettle, W. F.; Atkins, T. J. *Org. Synth.* **1978**, *58*, 86. (b) Searle, G. H.; Geue, R. J. *Aust. J. Chem.* **1984**, *37*, 959. (c) Chaudhuri, P.; Wieghardt, K. *Prog. Inorg. Chem.* **1987**, *35*, 329.
(14) Tanase, T.; Lippard, S. J. *Inorg. Chem.* **1995**, *34*, 4682.
(15) Tanase, T.; Yun, J. W.; Lippard, S. J. *Inorg. Chem.* **1995**, *34*, 4220.

Chemical shifts were calibrated to tetramethylsilane as an external reference. $^{13}C\{^1H\}$ NMR spectra were recorded on the same instruments at 75 MHz, chemical shifts being calibrated to tetramethylsilane as an external reference. Electron microprobe analyses for metal ions were carried out on a Shimadzu EPMA-2300 analyzer.

Preparation of [M{(D-Glc)$_2$-tacn}Cl]Cl (M = Zn (11), Cu (12), Ni (13), Co (14)). D-Glucose (1.08 g, 6.00 mmol), tacn (0.391 g, 3.00 mmol), and NH_4Cl (0.161 g, 3.00 mmol) were dissolved in 30 mL of methanol, and the solution was incubated at 65 °C for 5 h. After cooling to room temperature, a solution of $ZnCl_2$ (0.410 g, 3.00 mmol) in MeOH (45 mL) was slowly (over 2 h) added to the resultant solution, which was stirred at room temperature for ~12 h. The solution was concentrated to ca. 50 mL and then passed through a glass filter to remove inorganic salts. The concentrated solution was further allowed to stand at room temperature and to evaporate slowly to afford colorless crystals of [Zn{(D-Glc)$_2$-tacn}Cl]Cl·H_2O (**11**·H_2O), which were washed with ethanol and diethyl ether and dried under vacuum (Yield 76%). Anal. Calcd for $C_{18}H_{37}N_3O_{11}Cl_2Zn$: C, 35.57; H, 6.14; N, 6.91. Found: C, 35.49; H, 6.16; N, 7.08. IR (KBr): 3349 br, 1625 m, 1500, 1461, 1369, 1345, 1288, 1272, 1240, 1108, 1076 s, 1014, 988, 908, 817 cm^{-1}. $^{13}C\{^1H\}$ NMR (in CD_3OD): δ 94.9, 94.2 (C-1 of D-Glc), 80.9, 80.7, 78.1, 72.5, 72.2, 71.9, 71.5, 62.6, 57.4, 54.6 (C-2~6 of D-Glc), 42.8, 41.9, 41.2 (tacn). When 1-^{13}C enriched D-glucose ([1-^{13}C]-D-Glc) was used, [Zn{([1-^{13}C]-D-Glc)$_2$-tacn}Cl]Cl·H_2O (**11***·H_2O) was obtained in 25% yield; the IR spectrum showed a pattern similar to that of **11**. IR (KBr): 3349 br, 1625 m, 1499, 1461, 1369, 1345, 1289, 1270, 1238, 1107, 1075 s, 1051s, 1036 s, 1013, 907, 817 cm^{-1}.

Following the same procedure and using $CuCl_2$·$2H_2O$ (0.511 g, 3.00 mmol), pale blue microcrystals of [Cu{(D-Glc)$_2$-tacn}Cl]Cl·1.5H_2O (**12**·1.5H_2O) were obtained in 64% yield. Anal. Calcd for $C_{18}H_{38}N_3O_{11.5}Cl_2Cu$: C, 35.16: H, 6.23; N, 6.83. Found: C, 34.85; H, 6.01; N, 6.69. IR (KBr): 3365 br, 1628 m, 1457, 1380, 1346, 1285, 1269, 1242, 1123, 1080 s, 1041, 1005, 990, 907, 821 cm^{-1}. UV−Vis (in CH_3OH): ν_{max} (ϵ) 13.29 (65.4) $10^3 \times$ cm^{-1} (M^{-1}cm^{-1}). CD (in CH_3OH): ν_{max} ($\Delta\epsilon$) 14.92 (+0.504) $10^3 \times$ cm^{-1} (M^{-1} cm^{-1}). Recrystallization of the product from MeOH gave rectangular plates of **12**·H_2O. When the reaction solution was purified on a Sephadex LH-20 gel permeation column, pale blue needles of **12**·MeOH were obtained. An X-ray crystallographic analysis was carried out on **12**·MeOH.

By using $NiCl_2$·$6H_2O$, pale blue crystals of [Ni{(D-Glc)$_2$-tacn}Cl]-Cl·H_2O (**13**·H_2O) were obtained in 7% yield. Anal. Calcd for $C_{18}H_{37}N_3O_{11}Cl_2Ni$: C, 35.97; H, 6.20; N, 6.99. Found: C, 35.72; H, 6.33; N, 6.92. IR (KBr): 3286 br, 1628 m, 1458, 1400, 1347, 1288, 1268, 1238, 1122, 1077 s, 1053, 1011, 909, 828 cm^{-1}. UV−Vis (in CH_3OH): ν_{max} (ϵ) 16.65 (11.3), 26.21 (18.4) $10^3 \times$ cm^{-1} (M^{-1} cm^{-1}). CD (in CH_3OH): ν_{max} ($\Delta\epsilon$) 14.45^{sh} (-7.07×10^{-2}), 17.36 (-10.62×10^{-2}), 26.56 (-6.34×10^{-2}) $10^3 \times$ cm^{-1} (M^{-1} cm^{-1}).

A mixture of D-glucose (182 mg, 1.01 mmol), tacn (65.1 mg, 0.504 mmol), and NH_4Cl (27.0 mg, 0.505 mmol) in 10 mL of MeOH was heated at 65 °C for 3 h. The solution was cooled to room temperature, and a methanolic solution (10 mL) of $CoCl_2$·$6H_2O$ (120 mg, 0.505 mmol) was slowly added to the solution over 30 min. The mixture was stirred at room temperature for 4 h and chromatographed with a Sephadex LH-20 gel permeation column (2.6 × 34 cm). The purple main band was collected and concentrated to afford purple crystals of [Co{(D-Glc)$_2$-tacn}Cl]Cl·H_2O (**14**·H_2O) in 39% yield. Anal. Calcd for $C_{18}H_{37}N_3O_{11}Cl_2Co$: C, 35.95; H, 6.20; N, 6.99. Found: C, 36.18; H, 6.37; N, 6.94. IR (KBr): 3290 br, 1625 m, 1463, 1435, 1368, 1346, 1287, 1271, 1239, 1106, 1075 s, 1051, 1012, 906, 821 cm^{-1}. UV−Vis (in CH_3OH): ν_{max} (ϵ) 19.32 (32.7) $10^3 \times$ cm^{-1} (M^{-1} cm^{-1}). CD (in CH_3OH): ν_{max} ($\Delta\epsilon$) 17.94 (-0.565), 19.94^{sh} (-0.506) $10^3 \times$ cm^{-1} (M^{-1} cm^{-1}).

Preparation of [Ni{(L-Rha)$_2$-tacn}(MeOH)]Cl$_2$ (15). L-Rhamnose (0.547 g, 3.00 mmol) and tacn (128 mg, 0.994 mmol) were dissolved in 40 mL of methanol and heated at reflux for 1.5 h. After cooling the solution to room temperature, a methanolic solution (20 mL) containing $NiCl_2$·$6H_2O$ (238 mg, 1.00 mmol) was slowly added over 1h to the solution, which was stirred at room temperature overnight. The resultant solution was concentrated to ca. 10 mL and chromatographed with a Sephadex LH-20 gel permeation column (4 × 60 cm). The first eluted main blue band was collected and concentrated to ca. 5 mL. A small amount of Et_2O was added to the solution, which was allowed to stand at 2 °C, to afford pale blue needles of [Ni{(L-Rha)$_2$-tacn}(MeOH)]-Cl_2·MeOH (**15**·2MeOH) in 10% yield. Anal. Calcd for $C_{19}H_{45}N_3O_{12}Cl_2Ni$: C, 35.82; H, 7.12; N, 6.59. Found: C, 35.65; H, 7.38; N, 6.77. IR (KBr): 3425 br, 1633 m, 1491, 1455, 1388, 1355, 1298, 1265, 1242, 1094, 1059 s, 1029, 1008, 962, 899, 871, 830, 777, 717 cm^{-1}. UV−Vis (in CH_3OH): ν_{max} (ϵ) 17.05 (10.0), 26.89 (14.0) $10^3 \times$ cm^{-1} (M^{-1} cm^{-1}). CD (in CH_3OH): ν_{max} ($\Delta\epsilon$) 17.21 ($+18.7 \times 10^{-2}$), 26.25 ($+9.72 \times 10^{-2}$) $10^3 \times$ cm^{-1} (M^{-1} cm^{-1}).

Preparation of [Cu(XDK)(py)$_2$]·1.5CHCl$_3$ (22). To a solution of methanol (20 mL) containing Na_2XDK·$4H_2O$ (102 mg, 0.15 mmol) was added a methanolic solution (10 mL) of $Cu(NO_3)_2$·$3H_2O$ (36.5 mg, 0.15 mmol), and the reaction solution was stirred at room temperature for 30 min. Excess pyridine (~100 mg) was added to the solution, which was stirred for another 30 min. The solvent was removed under reduced pressure, and the residue was extracted with 30 mL of chloroform. The extract was passed through a glass filter and concentrated to ca. 2 mL. Diethyl ether (4 mL) was carefully added to the concentrated solution, which was kept in a refrigerator, to give block-shaped blue crystals of [Cu(XDK)(py)$_2$]·1.5$CHCl_3$ (**22**·1.5$CHCl_3$) in 89% yield. Anal. Calcd for $C_{43.5}H_{49.5}N_4O_8Cl_{4.5}Cu$: C, 53.34; H, 5.09; N, 5.72. Found: C, 52.99; H, 5.61; N, 5.98. IR (KBr): 1731, 1678 s, 1610, 1587 s, 1462, 1450, 1384, 1360, 1195, 1071, 958, 851, 763, 696 cm^{-1}. UV−Vis (in CH_3OH): ν_{max} (ϵ) 13.11 (59.6) $10^3 \times$ cm^{-1} (M^{-1} cm^{-1}). Recrystallization from CH_2Cl_2/Et_2O afforded large block-shaped crystals of **22**·CH_2Cl_2 suitable for X-ray crystallography.

Preparation of [Zn$_2$M{(D-Glc)$_2$-tacn}$_2$(XDK)]Cl$_2$ (M = Zn (31), Cu (32)). To 20 mL of a methanolic solution containing [Zn{(D-Glc)$_2$-tacn}Cl]Cl·H_2O (**11**·H_2O) (62.7 mg, 0.103 mmol) was added a solution (10 mL) of [Zn(XDK)(H_2O)] (**21**) (62.2 mg, 0.094 mmol) in methanol. After stirring at room temperature for 12 h, the solution was concentrated to ca. 1.5 mL. A small amount of diethyl ether (ca. 0.5 mL) was carefully added, and the resultant solution was allowed to stand in a refrigerator to afford colorless crystals of [Zn$_3${(D-Glc)$_2$-tacn}$_2$(XDK)]Cl_2·$9H_2O$ (**31**·$9H_2O$). The crystals were collected, washed with Et_2O, and dried under vacuum (yield 33%). Anal. Calcd for $C_{68}H_{124}N_8O_{37}Cl_2Zn_3$: C, 42.70; H, 6.53; N, 5.86; Cl, 3.71. Found: C, 42.72; H, 6.18; N, 6.20; Cl, 4.15. IR (KBr): 3398 br, 1725, 1683 s, 1564 s, 1489, 1464, 1424, 1404, 1383, 1364, 1200, 1115, 1077, 1050 s, 959, 896, 853, 813, 783, 766, 663 cm^{-1}. By using [Zn{([1-^{13}C]-D-Glc)-tacn}Cl]Cl·H_2O (**11***·H_2O), [Zn$_3${([1-^{13}C]-D-Glc)$_2$-tacn}$_2$(XDK)]-Cl_2·$8H_2O$ (**31***·$9H_2O$) was obtained; the IR spectrum was similar to that of **31**·$9H_2O$. IR (KBr): 3419 br, 1726, 1684 s, 1564 s, 1489, 1465, 1424, 1404, 1383, 1364, 1200, 1113, 1076, 1035 s, 959, 893, 853, 813, 780, 765, 663 cm^{-1}.

When [Cu(XDK)(py)$_2$]·1.5$CHCl_3$ (**22**·1.5$CHCl_3$) (81.2 mg (0.101 mmol) in MeOH (10 mL) was added to a methanolic solution (20 mL) of **11**·H_2O (50.3 mg, 0.083 mmol), pale blue crystals of [Zn$_2$Cu{(D-Glc)$_2$-tacn}$_2$(XDK)]Cl_2·$5H_2O$ (**32**·$5H_2O$) were obtained in 28% yield. Anal. Calcd for $C_{68}H_{116}N_8O_{33}Cl_2Zn_2Cu$: C, 44.41; H, 6.36; N, 6.09; Cl, 3.86. Found: C, 44.31; H, 5.92; N, 6.01; Cl, 4.20. The atomic existence ratio of Cu/Zn was 1.0:1.8 determined by an EPMA analysis. IR (KBr): 3400 br, 1726, 1685 s, 1560 s, 1490, 1464, 1424, 1404, 1384, 1364, 1200, 1122, 1077 s, 1046 s, 960, 891, 853, 814, 764, 672 cm^{-1}. UV−Vis (in CH_3OH): ν_{max} (ϵ) 12.95 (1.39×10^2) $10^3 \times$ cm^{-1} (M^{-1} cm^{-1}). CD (in CH_3OH): ν_{max} ($\Delta\epsilon$) 13.16 (+0.92), 11.12 (0.00), 10.48 (-0.13), 9.78 (0.00), 9.00 (+0.14) $10^3 \times$ cm^{-1} (M^{-1} cm^{-1}).

Preparation of [Cu$_2$M{(D-Glc)$_2$-tacn}$_2$(XDK)]Cl$_2$ (M = Cu (33), Zn (34)). To a methanolic solution (30 mL) containing [Cu{(D-Glc)$_2$-tacn}Cl]Cl·1.5H_2O (**12**·1.5H_2O) (49.6 mg, 0.082 mmol) was added [Cu(XDK)(py)$_2$]·1.5$CHCl_3$ (**22**·1.5$CHCl_3$) (81.3 mg, 0.102 mmol) dissolved in 10 mL of MeOH. The resultant solution was stirred at room temperature for 12 h, passed through a glass filter, and concentrated to ca. 0.5 mL. A small amount of Et_2O (0.5 mL) was carefully added to the concentrated solution to afford bluish green microcrystals of [Cu$_3${(D-Glc)$_2$-tacn}$_2$(XDK)]Cl_2·$7H_2O$ (**33**·$7H_2O$) in 23% yield. Anal. Calcd for $C_{68}H_{120}N_8O_{35}Cl_2Cu_3$: C, 43.65; H, 6.46; N, 5.99; Cl, 3.79. Found: C, 43.46; H, 6.05; N, 6.08; Cl, 4.08. IR (KBr): 3389 br, 1726, 1685 s, 1559 s, 1499, 1464, 1423, 1399, 1384, 1363, 1201, 1125, 1078 s, 1046 s, 987, 960, 895, 853, 812, 764, 676 cm^{-1}. UV−Vis (in CH_3OH): ν_{max} (ϵ) 12.90 (2.00×10^2) $10^3 \times$ cm^{-1} (M^{-1} cm^{-1}). CD (in CH_3OH): ν_{max}

Table 1. Crystallographic and Experimental Data for **11**·H_2O, **12**·MeOH, **13**·H_2O, and **14**·H_2O

compound	**11**·H_2O	**12**·MeOH	**13**·H_2O	**14**·H_2O
formula	$C_{18}H_{37}N_3O_{11}Cl_2Zn$	$C_{19}H_{39}N_3O_{11}Cl_2Cu$	$C_{18}H_{37}N_3O_{11}Cl_2Ni$	$C_{18}H_{37}N_3O_{11}Cl_2Co$
fw	607.79	619.98	601.11	601.34
cryst syst	monoclinic	monoclinic	monoclinic	monoclinic
space group	$P2_1$	$P2_1$	$P2_1$	$P2_1$
a/Å	10.942(3)	10.948(6)	10.899(7)	10.945(9)
b/Å	11.125(2)	11.160(4)	11.07(1)	10.976(4)
c/Å	11.064(5)	11.128(3)	10.040(4)	11.002(5)
β/deg	113.66(3)	113.30(2)	113.77(3)	113.83(5)
V/Å^3	1233.5(7)	1248.8(8)	1218(1)	1230(1)
Z	4	4	4	4
T/°C	−101	−118	−118	−118
d_{calcd}/g cm^{-1}	1.636	1.649	1.638	1.652
μ/cm^{-1}	12.75	11.52	10.78	9.94
scan method	$\omega - 2\theta$	$\omega - 2\theta$	$\omega - 2\theta$	$\omega - 2\theta$
scan speed/ deg min^{-1}	8	8	8	8
2θ max/deg	50	50	50	50
h,k,l range	$+h, +k, \pm l$	$+h, +k, \pm l$	$+h, +k, \pm l$	$+h, +k, \pm l$
no. of data	2307	2307	2268	2245
no. of obsd data	1861 ($I > 3\sigma(I)$)	2018 ($I > 2\sigma(I)$)	1537 ($I > 2\sigma(I)$)	1270 ($I > 1.5\sigma(I)$)
solution	direct methods SIR92	direct methods SIR92	direct methods SIR92	direct methods SIR92
no. of param	326	337	238	158
data/param	5.71	5.99	6.46	8.04
R^a	0.058	0.046	0.054	0.084
R_w [a]	0.065	0.050	0.056	0.086
GOF[b]	2.15	1.52	1.30	1.18

[a] $R = \sum||F_o| - |F_c||/\sum|F_o|$; $R_w = [\sum w(|F_o| - |F_c|)^2/\sum w|F_o|^2]^{1/2}$ ($w = 1/\sigma^2(F_o)$). [b] GOF $= [\sum w(|F_o| - |F_c|)^2/(N_o - N_p)]^{1/2}$ (N_o = no. data, N_p = no. variables).

($\Delta\epsilon$) 13.32 (+0.68), 12.15 (0.00), 10.67 (−1.60), 9.78 (0.00), 8.37 (+1.41) $10^3 \times$ cm^{-1} (M^{-1} cm^{-1}).

When **12**·1.5H_2O (101 mg, 0.17 mmol) was reacted with **21** (110 mg, 0.17 mmol) in methanol (40 mL), pale blue microcrystals of [Cu_2-Zn{(D-Glc)$_2$-tacn}$_2$(XDK)]Cl_2·8H_2O (**34**·8H_2O) were obtained in 34% yield. Anal. Calcd for $C_{68}H_{122}N_8O_{36}Cl_2Cu_2Zn$: C, 43.19; H, 6.50; N, 5.93; Cl, 3.75. Found: C, 43.16; H, 6.19; N, 5.99; Cl, 3.89. The atomic existence ratio of Zn/Cu was 1.0:1.9 determined by an EPMA analysis. IR (KBr): 3398 br, 1726, 1685 s, 1561 s, 1491, 1463, 1424, 1404, 1382, 1364, 1200, 1077 s, 1047 s, 959, 893, 853, 813, 765, 667 cm^{-1}. UV−Vis (in CH_3OH): ν_{max} (ϵ) 13.02 (1.39×10^2) $10^3 \times$ cm^{-1} (M^{-1} cm^{-1}). CD (in CH_3OH): ν_{max} ($\Delta\epsilon$) 13.18 (+1.08), 9.53 (0.00), 8.34 (−0.11) $10^3 \times$ cm^{-1} (M^{-1} cm^{-1}).

X-ray Crystallography. Crystals of **11**·H_2O, **12**·MeOH, **13**·H_2O, **14**·H_2O, **15**·2MeOH, **22**·CH_2Cl_2, **31**·4.5MeOH·3.5H_2O, and **34**·3.5MeOH·2H_2O were quickly coated with Paraton N oil and mounted on the tips of glass fibers at low temperature. Crystals of **16**·2MeOH, **22**·CH_2Cl_2, **31**·4.5MeOH·3.5H_2O, and **34**·3.5MeOH·2H_2O were extremely delicate when they were separated from their mother liquors. Crystal data and experimental conditions are summarized in Tables 1 and 2. All data were collected at −101 ∼ −140 °C on a Rigaku AFC7R diffractometer equipped with graphite monochromatized Mo Kα (λ = 0.71069 Å) radiation. Three standard reflections were monitored every 150 reflections and showed no systematic decrease in intensity. Reflection data were corrected for Lorentz polarization and absorption effects (ψ-scan method).

The structure of **11**·H_2O was solved by direct methods with SIR92.[16]Most of the non-hydrogen atoms were located initially, and subsequent cycles of Fourier syntheses and least-squares refinements gave the positions of other non-hydrogen atoms. The coordinates of C−H and N−H hydrogen atoms were calculated at ideal positions with a distance of 0.95 Å, and the coordinates of the O−H hydrogen atoms were determined by difference Fourier syntheses. The structure was refined with the full-matrix least-squares techniques on F minimizing $\sum w(|F_o| - |F_c|)^2$. Final refinement with anisotropic thermal parameters for non-hydrogen atoms converged at R values listed in Table 1. The hydrogen atoms were fixed in the refinement. The chloride counteranion was disordered and was refined using a two-site model, with occupancies being 0.6 for Cl(2) and 0.4 for Cl(3). The crystal structure of **13**·H_2O and **14**·H_2O were isomorphous with that of **11**·H_2O, and were solved and refined using a procedure similar to that described above. Final refinement was carried out with anisotropic thermal parameters for the Ni, Cl, O, and N atoms and with isotropic ones for the other non-hydrogen atoms for **13**·H_2O, and refinement for **14**·H_2O was carried out with anisotropic thermal parameters for the Co and Cl atoms and with isotropic ones for the other non-hydrogen atoms. The chloride counteranion was not disordered.

The structures of **12**·MeOH, **15**·2MeOH, and **22**·CH_2Cl_2 were solved and refined by a procedure similar to that for **11**·H_2O. Final refinements were carried out with anisotropic thermal parameters for non-hydrogen atoms. All hydrogen atoms were located by difference Fourier syntheses and were fixed in the refinements in **12**·MeOH and **15**·2MeOH. The positions of the C−H hydrogen atoms in **22**·CH_2Cl_2 were calculated at ideal positions and were not refined. The chloride counteranion was disordered and was refined using a two-site model with occupancies being 0.81 for Cl(2) and 0.19 for Cl(3) in **12**·MeOH.

The structure of **31**·4.5MeOH·3.5H_2O was solved by direct methods with SIR92 and was refined with full-matrix least-squares techniques. The coordinates of C−H and N−H hydrogen atoms, except those of solvents, were calculated at ideal positions with a distance of 0.95 Å and were not refined. Final refinement with anisotropic thermal parameters for the Zn and Cl atoms and with isotropic ones for other non-hydrogen atoms converged at the R values listed in Table 2. The solvent molecules were disordered and refined as 4.5MeOH and 3.5H_2O. The structure of **34**·3.5MeOH·2H_2O was isomorphous to that of **31**·4.5MeOH·3.5H_2O, and it was solved and refined by a method similar to that described above. The coordinates of C−H and N−H hydrogen atoms, except those of solvents ,were calculated at ideal positions and were not refined. Final refinement was carried out with anisotropic thermal parameters for all non-hydrogen atoms except those of solvent molecules. The solvent molecules were considerably disordered and refined as 3.5MeOH and 2H_2O with isotropic temperature factors.

The absolute configurations of all the chiral crystal structures were determined using the known configurations of sugars as internal references. Atomic scattering factors and values of f' and f'' for Zn,

(16) Burla, M. C.; Camalli, M.; Cascarano, G.; Giacovazzo, C.; Polidori, G.; Spagna, R.; Viterbo, D. *J. Appl. Crystallogr.* **1989**, *22*, 389.

Table 2. Crystallographic and Experimental Data for **15**·2MeOH, **22**·CH_2Cl_2, **31**·4.5MeOH·3.5H_2O, and **34**·3.5MeOH·2H_2O

compound	**15**·2MeOH	**22**·CH_2Cl_2	**31**·4.5MeOH·3.5H_2O	**34**·3.5MeOH·2H_2O
formula	$C_{21}H_{47}N_3O_{11}Cl_2Ni$	$C_{43}H_{50}N_4O_8Cl_2Cu$	$C_{72.5}H_{129}N_8O_{36}Cl_2Zn_3$	$C_{71.5}H_{126}N_8O_{34.5}Cl_2Cu_2Zn$
fw	647.22	885.34	1955.89	1913.21
cryst syst	monoclinic	monoclinic	orthorhombic	orthorhombic
space group	$P2_1$	$P2_1/n$	$P2_12_12_1$	$P2_12_12_1$
a/Å	8.297(4)	14.065(4)	19.235(5)	19.229(5)
b/Å	11.376(5)	22.531(6)	31.15(1)	31.347(8)
c/Å	15.186(4)	13.356(4)	15.753(6)	15.751(4)
β/deg	99.66(3)	90.23(3)		
V/Å^3	1413.0(9)	4232(1)	9438(4)	9494(3)
Z	4	4	4	4
T/°C	−101	−130	−118	−117
d_{calcd}/g cm^{-1}	1.521	1.389	1.376	1.339
μ/cm^{-1}	9.36	6.99	8.98	8.23
scan method	$\omega - 2\theta$	$\omega - 2\theta$	$\omega - 2\theta$	$\omega - 2\theta$
scan speed/ deg min^{-1}	8	8	8	8
2θ max/°	50	50	50	50
h,k,l range	$+h, +k, \pm l$	$+h, +k, \pm l$	$+h, +k, +l$	$+h, +k, +l$
no. of data	2612	7445	9039	8949
no. of obsd data	2264 ($I > 2\sigma(I)$)	4252 ($I > 2\sigma(I)$)	4236 ($I > 3\sigma(I)$)	6488 ($I > 2\sigma(I)$)
solution	direct methods SIR92	direct methods SIR92	direct methods SIR92	direct methods SIR92
no. of param	344	524	520	1040
data/param	6.58	8.11	8.15	6.24
R^a	0.042	0.061	0.077	0.070
$R_w{}^a$	0.048	0.073	0.088	0.078
GOF^b	1.38	1.57	1.87	2.37

[a] $R = \sum||F_o| - |F_c||/\sum|F_o|$; $R_w = [\sum w(|F_o| - |F_c|)^2/\sum w|F_o|^2]^{1/2}$ ($w = 1/\sigma^2(F_o)$). [b] GOF $= [\sum w(|F_o| - |F_c|)^2/(N_o - N_p)]^{1/2}$ (N_o = no. data, N_p = no. variables).

Cu, Ni, Co, Cl, O, N, and C were taken from the literature.[17] All calculations were carried out on Silicon Graphics Indigo and O2 Stations with the teXsan program package.[18] The perspective views were drawn using the program ORTEP.[19] Compilation of final atomic parameters for all non-hydrogen atoms is supplied as Supporting Information.

EXAFS Analysis. X-ray absorption measurements at the Zn K edge (8960−11160 eV with 677 steps) were performed at the Photon Factory of the National Laboratory for High Energy Physics on beam line 10B using synchrotron radiation (2.5 GeV, 300−270 mA).[20] Experiments were performed in the transmission mode on powdered samples (BN pellets) of **11** and **31** and a solution sample of **31** (~0.1 M in DMF), at room temperature using a Si(311) monochromator. The theoretical expression for $\boldsymbol{k}^3\chi(\boldsymbol{k})$ for the case of single scattering is given by eq 1, where $\boldsymbol{r}_i$, N_i, S_i, $F_i(\boldsymbol{k})$, $\Phi_i(\boldsymbol{k})$, and σ_i represent the interatomic distance, the coordination number, the reducing factor, the backscattering amplitude, the phase shift, and the Debye−Waller factor, respectively, and $\boldsymbol{k}$ is the photoelectron wave vector defined as $\boldsymbol{k} = [(2m/\hbar^2)(E - E_0)]^{1/2}$ (E_0 = 9657 keV).[21] The backscattering amplitude $F_i(\boldsymbol{k})$ and the phase shift $\Phi_i(\boldsymbol{k})$ functions used were the theoretical parameters tabulated by McKale et al.[22] Parameters, N_i, $\boldsymbol{r}_i$, E_0, and σ_i were varied in the nonlinear least-squares refined curve fitting with fixed values of S_i. The reducing factors S_i are determined from the analysis of **31** (powder). Fourier filtered ($\boldsymbol{r}$ = 1.1−3.5 Å before phase-shift correction) EXAFS data, $\boldsymbol{k}^3\chi(\boldsymbol{k})_{obsd}$, were analyzed with three waves, $\boldsymbol{k}^3\chi(\boldsymbol{k})_{calcd} = \boldsymbol{k}^3\chi_{N/O} + \boldsymbol{k}^3\chi_C + \boldsymbol{k}^3\chi_{Zn}$, in a $\boldsymbol{k}$ space of 2−13 Å^{-1} for complex **31** and with four waves, $\boldsymbol{k}^3\chi(\boldsymbol{k})_{calcd} = \boldsymbol{k}^3\chi_{N/O} + \boldsymbol{k}^3\chi_{Cl} + \boldsymbol{k}^3\chi_O + \boldsymbol{k}^3\chi_C$, for complex **11**. The first coordination sphere atoms, N/O, were treated as oxygen. All calculations were performed on an Hewlett-Packard Work Station Model 712/60 with the EXAFS analysis program package, REX (Rigaku Co. Ltd.).[23]

$$\boldsymbol{k}^3\chi(\boldsymbol{k}) = \sum_i \left(\frac{\boldsymbol{k}^2 N_i}{\boldsymbol{r}_i^2} S_i F_i(\boldsymbol{k}) \exp(-2\sigma_i^2 k^2) \sin(2\boldsymbol{k}\boldsymbol{r}_i + \Phi_i(k)) \right) \quad (1)$$

Results and Discussion

Mononuclear Complexes with D-Glucose, [M{(D-Glc)$_2$-tacn}Cl]Cl, M = Zn (11), Cu (12), Ni (13), Co (14). Reactions of $M^{II}Cl_2 \cdot nH_2O$ with *N*,*N*′-bis(D-glucopyranosyl)-1,4,7-triazacyclononane ((D-Glc)$_2$-tacn), formed from tacn and D-glucose in refluxing methanol, afforded a series of the mononuclear divalent metal complexes with the bis(*N*-β-D-glucopyranosyl)-amine ligand. The compounds [M^{II}\{(D-Glc)$_2$-tacn\}Cl]Cl, M = Zn (**11**), Cu (**12**), Ni (**13**), Co (**14**), were obtained in 7−76% yields (Scheme 1). Elemental analyses indicated that **11**−**14** had one tacn ligand, two sugar units, and two chloride anions per metal ion. IR spectra of the complexes closely resembled one another. In the CD spectra of **12**−**14**, Cotton effects were observed at the d−d transition wavelengths, and in the ^{13}C-\{^{1}H\} NMR spectrum of **11**, two sets of peaks for D-glucose appeared around 54−95 ppm. Resonances at δ 94.9 and 94.2 were assignable to the C-1 carbon atoms of the two inequivalent β-D-glucopyranosyl moieties.

X-ray crystallographic analyses of **11**−**14** indicated that they are isostructural, with a divalent metal cation surrounded by a [N_3O_2Cl] donor set. An ORTEP plot for the cationic complex in **11** (M = Zn) is illustrated in Figure 3 together with the atom numbering scheme,[24] and selected bond distances and angles for **11**−**14** are summarized in Table 3. In **11**, there is a

(17) (a) Cromer, D. T. *Acta Crystallogr.* **1965**, *18*, 17. (b) Cromer, D. T.; Waber, J. T. *International Tables for X-ray Crystallography*; Kynoch Press: Birmingham, England, 1974.
(18) TEXSAN Structure Analysis Package, Molecular Structure Corporation, the Woodsland, TX, 1985.
(19) Johnson, C. K. Oak Ridge National Laboratory: Oak Ridge, TN, 1976.
(20) *Photon Factory Activity Report*; National Laboratory for High Energy Physics: Ibaraki, Japan, 1986.
(21) Sayers, D. E.; Stern, E. A.; Lytle, F. W. *Phys. Rev. Lett.* **1971**, *27*, 1204.
(22) McKale, A. G.; Veal, B. W.; Paulikas, A. P.; Chan, S. K.; Knapp, G. S. *J. Am. Chem. Soc.* **1988**, *110*, 3763.
(23) Kosugi, N.; Kuroda, H. *REX*; Research Center for Spectrochemistry, the University of Tokyo: Tokyo, Japan, 1985.
(24) ORTEP diagrams for the complex cations of **12**−**14** are supplied as Supporting Information. The same atomic numbering system is applied for complexes **11**−**14**.

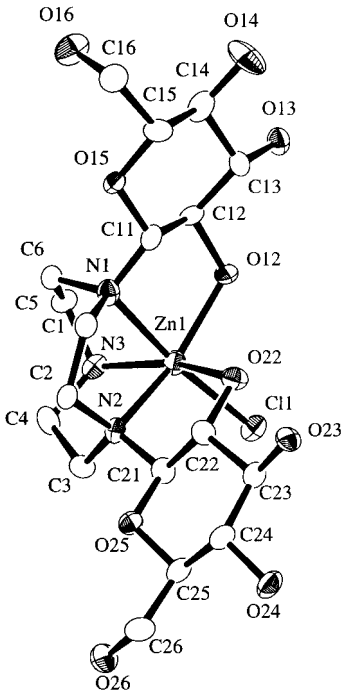

Figure 3. ORTEP plot of the complex cation of **11**, [Zn{(D-Glc)$_2$-tacn}Cl]Cl.

Scheme 1

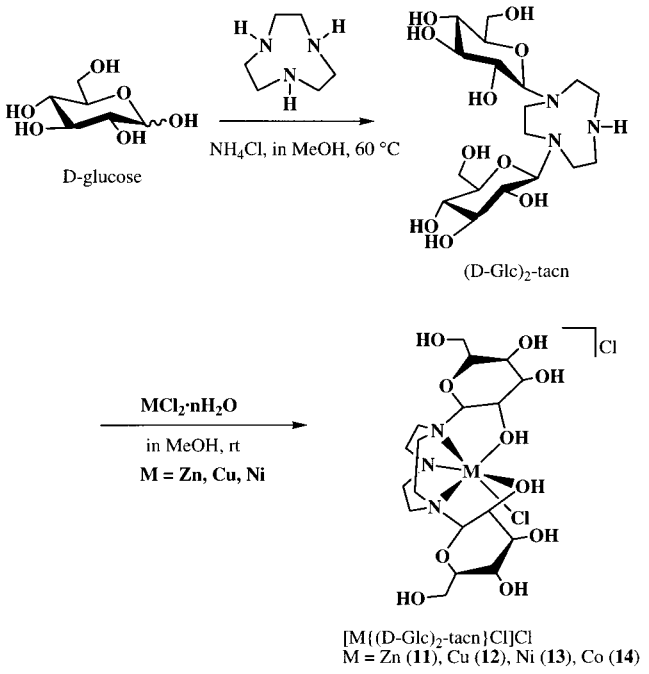

mononuclear Zn^{2+} ion ligated by the pentadentate *N*-glycoside ligand, (D-Glc)$_2$-tacn, and a chloride anion (Zn(1)−Cl(1) = 2.314(3) Å) with considerably distorted octahedral geometry. The smallest cis and trans angles are 74.6(3)° for O(22)−Zn(1)−N(2) and 157.5(3)° for O(22)−Zn(1)−N(3), respectively. Two D-glucose molecules are tethered to the N atoms of the face-capping tacn ligand through the β-glycosidic bond. They coordinate to the metal via the amino group at the anomeric position and the C-2 hydroxyl group to form five-membered chelate rings having a λ-gauche conformation. Both of the two β-D-glucosylamine moieties adopt the stable $^4C_1$ chair form with all donor atoms oriented equatorially; however, they exhibit somewhat different coordination behavior. The Zn(1)−O(22) bond length of 2.449(8) Å is significantly longer than the Zn(1)−O(12) distance of 2.121(6) Å, and the bite angle of O(22)−Zn(1)−N(2), 74.6(3)°, is smaller than that of O(12)−Zn(1)−N(1), 79.7(3)°. These structural parameters indicate that one sugar unit binds to the metal more strongly than the other one. The absolute configuration around the metal is Λ. The structure of complex **12** (M = Cu) is further distorted from idealized octahedral symmetry due to the usual Jahn−Teller effect. The axial positions are occupied by O(22) and N(3), with Cu(1)−O(22) = 2.601(6) Å and Cu(1)−N(3) = 2.184(7) Å. The structures of complexes **13** (M = Ni) and **14** (M = Co) are less distorted than those of **11** and **12**, although the M(1)−O(22) bond lengths of 2.275(9) (**13**) and 2.29(2) Å (**14**) are appreciably longer than the M(1)−O(12) bond lengths of 2.075(7) (**13**) and 2.10(1) Å (**14**).

Table 3. Selected Bond Lengths and Angles of [M{(D-Glc)$_2$-tacn}Cl]Cl (M = Zn (**11**), Cu (**12**), Ni (**13**), Co (**14**))[a]

	M = Zn (**11**)	M = Cu (**12**)	M = Ni (**13**)	M = Co (**14**)
Bond Lengths (Å)				
M(1)−Cl(1)	2.314(3)	2.266(3)	2.360(5)	2.348(8)
M(1)−O(12)	2.121(6)	2.047(5)	2.075(7)	2.10(1)
M(1)−O(22)	2.449(8)	2.601(6)	2.275(9)	2.29(2)
M(1)−N(1)	2.195(9)	2.049(7)	2.08(1)	2.16(2)
M(1)−N(2)	2.139(8)	2.072(7)	2.089(9)	2.16(2)
M(1)−N(3)	2.095(9)	2.184(7)	2.07(1)	2.08(2)
Bond Angles (°)				
Cl(1)−M(1)−O(12)	94.2(2)	92.4(2)	91.7(3)	95.0(5)
Cl(1)−M(1)−O(22)	88.5(2)	87.1(1)	89.0(3)	88.4(4)
Cl(1)−M(1)−N(1)	173.4(2)	175.4(2)	174.3(3)	175.1(5)
Cl(1)−M(1)−N(2)	104.0(2)	99.2(2)	101.2(3)	103.5(5)
Cl(1)−M(1)−N(3)	102.4(3)	99.7(2)	94.6(3)	98.1(6)
O(12)−M(1)−O(22)	92.0(3)	94.0(2)	94.0(3)	94.0(5)
O(12)−M(1)−N(1)	79.7(3)	83.6(3)	83.0(4)	80.2(6)
O(12)−M(1)−N(2)	156.9(3)	162.2(3)	165.1(5)	158.8(8)
O(12)−M(1)−N(3)	106.5(3)	107.1(2)	101.0(4)	103.5(6)
O(22)−M(1)−N(1)	89.1(3)	90.9(2)	93.4(4)	92.6(7)
O(22)−M(1)−N(2)	74.6(3)	73.3(2)	78.7(3)	76.6(6)
O(22)−M(1)−N(3)	157.5(3)	157.4(2)	164.4(4)	160.7(6)
N(1)−M(1)−N(2)	81.3(3)	84.2(3)	84.4(4)	81.4(7)
N(1)−M(1)−N(3)	81.9(3)	83.7(3)	84.5(4)	82.5(7)
N(2)−M(1)−N(3)	83.6(3)	84.3(3)	85.6(4)	84.2(6)
M(1)−O(12)−C(12)	114.2(6)	111.7(4)	110.3(6)	114(1)
M(1)−O(22)−C(22)	109.2(6)	106.3(4)	110.0(6)	110(1)

[a] Estimated standard deviations are given in parentheses.

Since the mononuclear bis-sugar complexes **11**−**14** have a labile coordination site, because the Cl^- anion is expected to be readily replaced by other ligands, they could be good building blocks for constructing multimetallic centers bridged by D-glucose moieties. At present, we have not been successful in obtaining a mono-sugar complex, formulated as [M{(D-Glc)-tacn}Cl$_2$], or tris-sugar complexes of [M{(D-Glc)$_3$-tacn}]Cl$_2$.

Mononuclear Nickel Complex with L-Rhamnose, [Ni{(L-Rha)$_2$-tacn}(MeOH)]Cl$_2$ (15). Other aldoses were examined in attempts to prepare sugar complexes. Only in the case of L-rhamnose (6-deoxy-L-mannose) and the nickel(II) ion were we able to obtain a crystalline compound of the bis-sugar complex, [Ni{(L-Rha)$_2$-tacn}(MeOH)]Cl$_2$ (**15**) (Scheme 2). Its structure was determined by X-ray crystallography, and an ORTEP diagram of the complex cation of **15,** along with the atomic numbering scheme, is illustrated in Figure 4. Selected bond lengths and angles are listed in Table 4. The nickel ion is octahedrally coordinated by the *N*,*N*′-bis(β-L-rhamnopyranosyl)-1,4,7-triazacyclononane ligand, (L-Rha)$_2$-tacn, and a methanol molecule. Three amino groups of the tacn ligand which anchors two β-L-rhamnosyl moieties just as observed in complexes **11**−**14** occupy a facial site of the octahedron. The other facial site

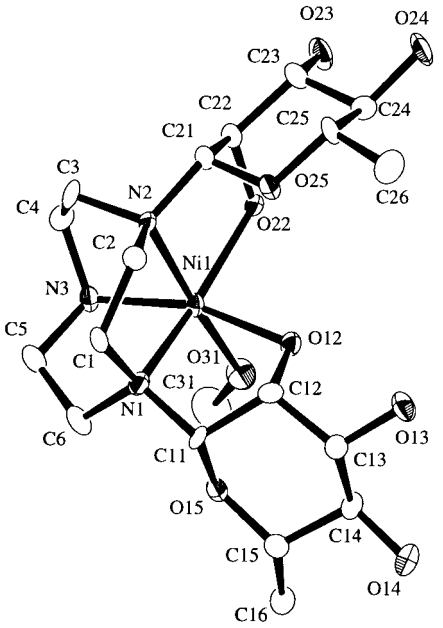

Figure 4. ORTEP plot of the complex cation of **15**, [Ni{(L-Rha)$_2$-tacn}(MeOH)]Cl$_2$.

Scheme 2

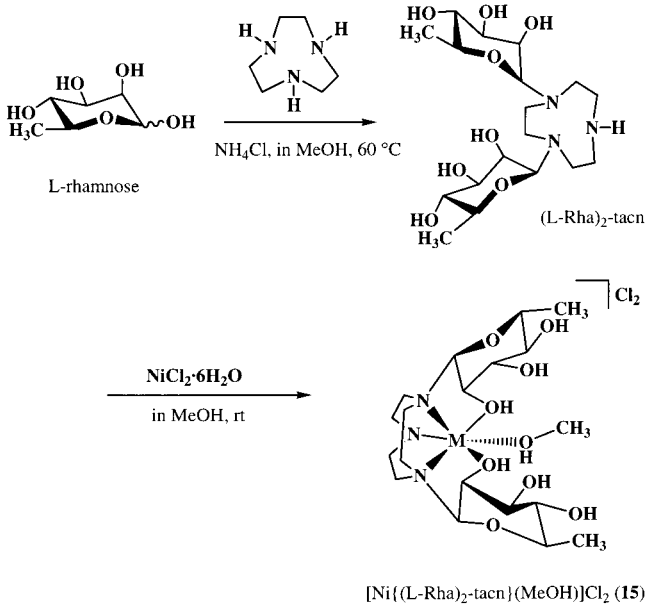

[Ni{(L-Rha)$_2$-tacn}(MeOH)]Cl$_2$ (**15**)

is coordinated by the two C-2 hydroxyl groups of the sugars and the methanol hydroxyl group. The two [NiNCCO] five-membered chelate rings assume λ-gauche conformations, and the absolute configuration around the metal is Λ. The two L-rhamnopyranosyl rings are directed toward the O_3 facial site, due to the axial orientation of the C-2 hydroxyl group, where they interact with each other by hydrogen bonding between the O(12) and O(25) atoms (2.907(6) Å). These arrangements lead to the formation of a sugar-coated hydrophilic site, to which two chloride counterions and a lattice methanol molecule are loosely associated through hydrogen bonding. Similar structures were observed in [Ni{(D-Man)$_2$-tren}]$^{2+}$ and [Ni{(L-Rha)$_2$-tren}]$^{2+}$, where (D-Man)$_2$-tren is bis(*N*-β-D-mannosyl-2-aminoethyl)(2-aminoethyl)amine and (L-Rha)$_2$-tren is bis(*N*-β-L-rhamnosyl-2-aminoethyl)(2-aminoethyl)amine.[4a]

Preparation of [Cu(XDK)(py)$_2$] (22). In previous work, the dinucleating biscarboxylate ligand XDK (H_2XDK = *m*-xylylenediamine bis(Kemp's triacid imide)) proved to be remarkably useful for stabilizing a variety of dimetallic centers.[14,15,25,26] In particular, the mononuclear zinc(II) XDK complex, [Zn(XDK)(H_2O)] (**21**), is a good precursor for zinc-containing heterodimetallic complexes, reacting with M(acac)$_2$ to afford a series of [MZn(XDK)(acac)$_2$(MeOH)$_2$] (M = Zn^{II}, Ni^{II}, Co^{II}, Fe^{II}, and Mn^{II}) complexes.[26] The related Cu(II) precursor, [Cu(XDK)(py)$_2$] (**22**), was prepared in the present study, and we have tried to use it to construct multinuclear metal centers bridged by D-glucose and carboxylate ligands by adopting the same strategy.

Table 4. Selected Bond Distances (Å) and Angles (deg) for **15**·2MeOH[a]

bond distances			
Ni(1)−O(12)	2.098(3)	Ni(1)−O(22)	2.134(4)
Ni(1)−O(31)	2.063(4)	Ni(1)−N(1)	2.085(5)
Ni(1)−N(2)	2.080(5)	Ni(1)−N(3)	2.057(5)
bond angles			
O(12)−Ni(1)−O(22)	94.4(1)	O(12)−Ni(1)−O(31)	84.0(2)
O(12)−Ni(1)−N(1)	79.9(2)	O(12)−Ni(1)−N(2)	101.6(2)
O(12)−Ni(1)−N(3)	163.1(2)	O(22)−Ni(1)−O(31)	92.4(2)
O(22)−Ni(1)−N(1)	162.8(2)	O(22)−Ni(1)−N(2)	80.6(2)
O(22)−Ni(1)−N(3)	102.0(2)	O(31)−Ni(1)−N(1)	103.1(2)
O(31)−Ni(1)−N(2)	171.2(2)	O(31)−Ni(1)−N(3)	91.0(2)
N(1)−Ni(1)−N(2)	84.7(2)	N(1)−Ni(1)−N(3)	85.5(2)
N(2)−Ni(1)−N(3)	85.4(2)		

[a] Estimated standard deviations are given in parentheses.

Complex **22** was prepared by the reaction of Na_2XDK·4H_2O with Cu(NO$_3$)$_2$·3H_2O in the presence of pyridine in good yield and was characterized by X-ray crystallography. An ORTEP plot with the atomic numbering scheme is given in Figure 5 and some selected bond lengths and angles are listed in Table 5. The Cu^{2+} ion is ligated by the two carboxylate oxygen atoms of XDK (Cu(1)−O(101) = 1.938(4) Å, Cu(1)−O(201) = 1.889(4) Å) and the two nitrogen atoms of pyridine molecules (Cu(1)−N(1) = 2.105(5) Å, Cu(1)−N(2) = 2.000(5) Å). It weakly interacts with the O(102) atom (2.321(4) Å), resulting in a considerably distorted trigonal bipyramidal geometry with O(101)−Cu(1)−O(201) = 168.7(2)° and N(1)−Cu(1)−N(2) = 120.5(2)°. There is no bonding interaction between Cu(1) and O(202) (3.114(5) Å).

Trimetallic Complexes Bridged by D-Glucose and Carboxylate Ligands. Reactions of [Zn{(D-Glc)$_2$-tacn}Cl]Cl (**11**) with [Zn(XDK)(H_2O)] (**21**) or [Cu(XDK)(py)$_2$] (**22**) in methanol at room temperature afforded colorless or pale blue crystals formulated as [Zn$_2$M′{(D-Glc)$_2$-tacn}$_2$(XDK)]Cl$_2$ (M′ = Zn (**31**), Cu (**32**)) in 28−33% yield (Scheme 3). When [Cu{(D-Glc)$_2$-tacn}Cl]Cl (**12**) was used instead of **11**, the analogous complexes, [Cu$_2$M′{(D-Glc)$_2$-tacn}$_2$(XDK)]Cl$_2$ (M′ = Zn (**33**), Cu (**34**)), were obtained as crystalline compounds in 23−34% yield (Scheme 3). Elemental analyses indicated that four D-glucose, two tacn, and one XDK ligands and two chloride anions were involved in the M$_2$M′ trinuclear metal ions. The IR spectra of

(25) (a) Goldberg, D. P.; Watton, S. P.; Masschelein, A.; Wimmer, L.; Lippard, S. J. *J. Am. Chem. Soc.* **1993**, *115*, 5346. (b) Watton, S. P.; Masschelein, A. Rebek, J., Jr.; Lippard, S. J. *J. Am. Chem. Soc.* **1994**, *116*, 5196. (c) Hagen, K. S.; Lachicotte, R.; Kitaygorodskiy, A.; Elbouadili, A. *Angew. Chem., Int. Ed. Engl.* **1993**, *32*, 1321. (d) Hagen, K. S.; Lachicotte, R.; Kitaygorodskiy, A. *J. Am. Chem. Soc.* **1993**, *115*, 12617. (e) Yun, J. W.; Tanase, T.; Pence, L. E.; Lippard, S. J. *J. Am. Chem. Soc.* **1995**, *117*, 4407. (f) Yun, W. J.; Tanase, T.; Lippard, S. J. *Inorg. Chem.* **1996**, *35*, 7590. (g) Herold, S.; Lippard, S. J. *J. Am. Chem. Soc.* **1997**, *119*, 145. (h) LeCloux, D. D.; Lippard, S. J. *Inorg. Chem.* **1997**, *36*, 4035. (i) He, C.; Lippard. S. J. *J. Am. Chem. Soc.* **1998**, *120*, 105.

(26) (a) Tanase, T.; Watton, S. P.; Lippard, S. J. *J. Am. Chem. Soc.* **1994**, *116*, 9401. (b) Tanase, T.; Yun, J. W.; Lippard, S. J. *Inorg. Chem.* **1996**, *35*, 3585.

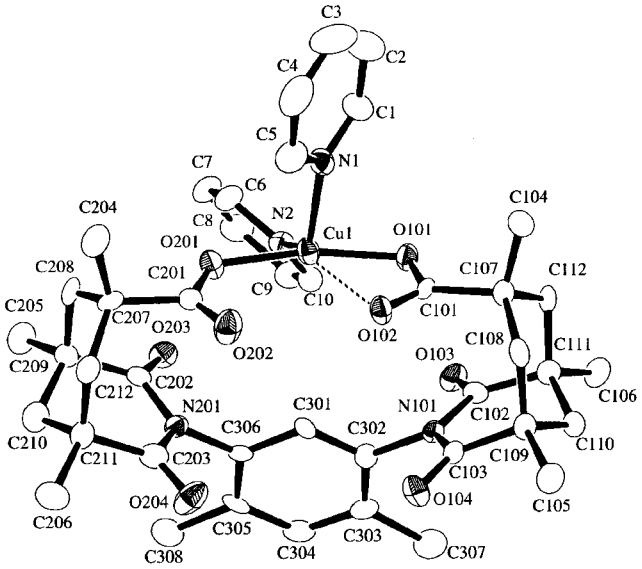

Figure 5. ORTEP plot of the complex **22**, $[Cu(XDK)(py)_2]$.

Table 5. Selected Bond Distances (Å) and Angles (Deg) for **22**·CH_2Cl_2[a]

bond distances			
Cu(1)−O(101)	1.938(4)	Cu(1)−O(201)	1.889(4)
Cu(1)···O(102)	2.321(4)		
Cu(1)−N(1)	2.105(5)	Cu(1)−N(2)	2.000(5)
O(101)−C(101)	1.282(7)	O(102)−C(101)	1.244(7)
O(201)−C(201)	1.274(7)	O(202)−C(201)	1.236(8)
bond angles			
O(101)−Cu(1)−O(201)	168.7(2)	O(101)−Cu(1)−N(1)	93.1(2)
O(101)−Cu(1)−N(2)	92.9(2)	O(201)−Cu(1)−N(1)	95.0(2)
O(201)−Cu(1)−N(2)	89.7(2)	N(1)−Cu(1)−N(2)	120.5(2)
Cu(1)−O(101)−C(101)	97.1(4)	Cu(1)−O(201)−C(201)	124.6(4)

[a] Estimated standard deviations are given in parentheses.

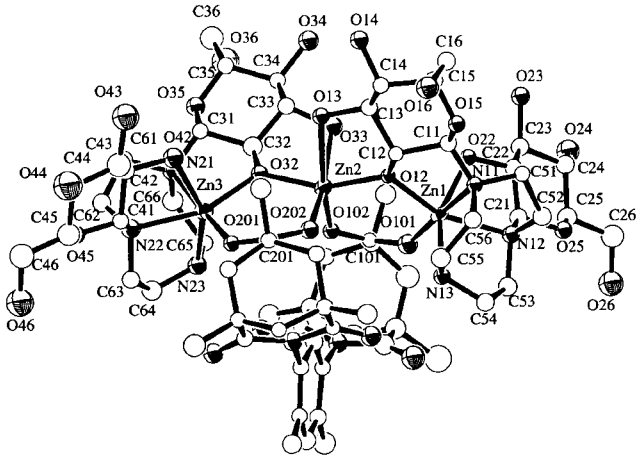

Figure 6. ORTEP plot of the complex cation of **31**, $[Zn_3\{(D\text{-}Glc)_2\text{-}tacn\}_2(XDK)]Cl_2$.

31−**34** closely resemble each other, showing the presence of the carbohydrate, XDK, and tacn ligands. The CD spectra of **32** (Zn_2Cu), **33** (Cu_3), and **34** (Cu_2Zn) in methanol exhibit broad positive Cotton effects in the d−d transition region (∼780 nm). No dinuclear complexes bridged by a XDK ligand were obtained under the reaction conditions.

The structures of **31** ($M'_2M = Zn_3$) and **34** ($M'_2M = Cu_2Zn$) were determined by crystallographic analysis. ORTEP plots of the complex cations with the atomic numbering schemes are illustrated in Figures 6 (**31**) and 7 (**34**), and selected bond distances and angles are listed in Tables 6 and 7. The crystal

Scheme 3

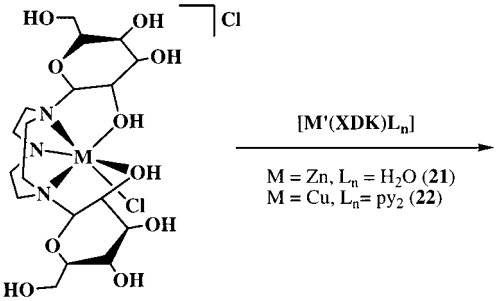

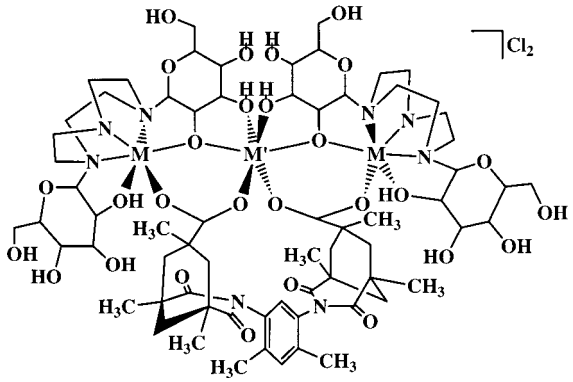

M = M' = Zn (**31**), M = Zn, M' = Cu (**32**)
M = M' = Cu (**33**), M = Cu, M' = Zn (**34**)

structures of **31** and **34** are isomorphous, with the asymmetric unit containing one complex cation and two chloride anions as well as solvent molecules of crystallization. The complex cation comprises three divalent metal ions, one biscarboxylate XDK ligand, and two deprotonated *N*-glycosides, $[(D\text{-}Glc)_2\text{-}tacn]^-$. In other words, the complexes can be regarded as two sugar-containing metal fragments, $[M'\{(D\text{-}Glc)_2\text{-}tacn\}]^+$ (M = Zn or Cu), which are joined by the {Zn(XDK)} unit. The terminal M atoms have a distorted octahedral geometry formed by the (D-Glc)$_2$-tacn ligand, through two oxygen atoms and three nitrogen atoms, and a carboxylate oxygen atom of XDK. The central M′ atoms assume significantly distorted octahedral structures, being ligated by four oxygen atoms of bridging carbohydrate residues in the $[(D\text{-}Glc)_2\text{-}tren]^-$ ligands and two carboxylate oxygen atoms of XDK. On the basis of the EPMA analysis for metal ions and the structural symmetry of complex **34**, the terminal metal sites are assigned as Cu^{2+} ions and the central one as a Zn^{2+} ion, in complex **34**. The appreciable Jahn−Teller distortion observed in **12** (M = Cu) was also present at the terminal metal centers, especially by comparison to the corresponding geometry in **31**.

The average M′···M separations are 3.440(4) (**31**) and 3.437(1) Å (**34**). Each MM′ dimetallic pair is bridged by a carboxylate group of XDK and the C-2 alkoxo group of a D-glucose moiety. Structurally characterized examples of carbohydrates bridging two metal centers are extremely rare, since isolation and characterization of such discrete molecules is very difficult owing to polymerization and their hygroscopic nature. As mentioned in the Introduction, however, mannose-type aldoses with the 2,3-cis-configuration, mannose, rhamnose, and lyxose so on, act as efficient bridging ligands in their β-furanose form, as reported for $[Ni_2(N,N'\text{-}(D\text{-}Man)_2{-}N,N'\text{-}Me_2en)(N{-}(D\text{-}Man)\text{-}N,N'\text{-}Me_2en)(CH_3OH)]Cl_2$ (**1**),[8] $Ba_2[M^{III}_2(\beta\text{-}D\text{-}mannose^{5-})_2]$ (**2**)[10] (M = Fe, V, Cr, Al, Ga), and $[Mo^{VI}_2O_4(\mu\text{-}O)(D\text{-}lyxose^{2-})]$ (**3**).[11] Recently, bridged structures of mannose-type aldoses with

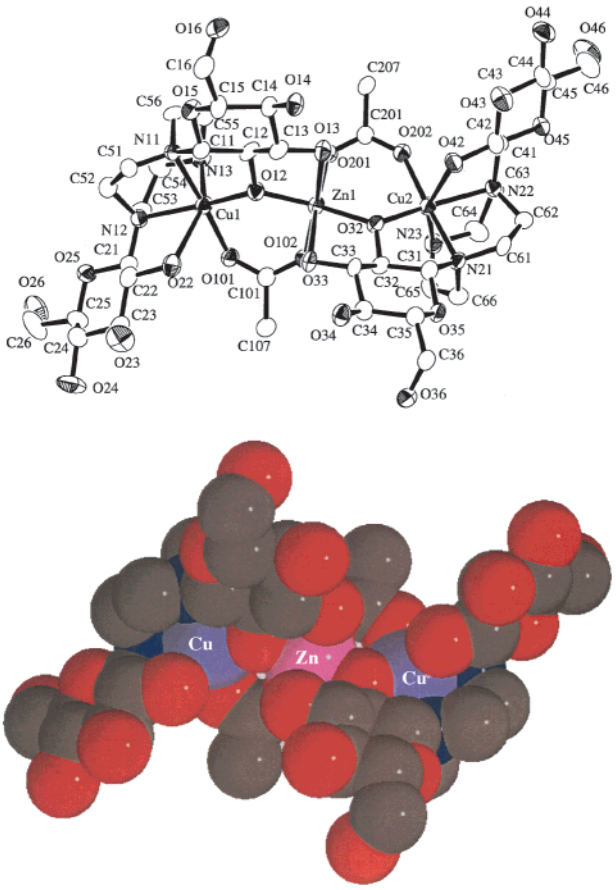

Figure 7. (a) ORTEP plot of the cluster core of **34**, $[Cu_2Zn\{(D\text{-Glc})_2\text{-tacn}\}_2(XDK)]Cl_2$, viewed along the pseudo C_2 axis. (b) Perspective drawing of the cluster core of **34** with van der Waals radii.

β-pyranosyl forms were also characterized in $[\{Mn((aldose_3\text{-tren}^{2-})\}_2Mn(H_2O)]^{3+}$ (**4**)[7c] (aldose$_3$-tren = tris(*N*-aldopyranosyl-2-aminoethyl)amine, and aldose = D-mannose, L-rhamnose) and $[\{V(=O)_2(\text{methyl } O\text{-4,6-benzylidene-}\alpha\text{-D-mannopyranoside}^{2-})\}_2$ (**5**).[27] In contrast, no structurally characterized examples of a D-glucose-bridged dimetallic center has been reported to date. The major reason for this deficiency may be that the glucose-type aldoses with a 2,3-trans configuration have a low affinity for metal ions because all of the hydroxyl groups are in mutually trans arrangements and dispersed in equatorial directions, with respect to the pyranoid ring.[28] Complexes **31** and **34** are the first characterized examples where a D-glucopyranosyl moiety bridges two metal ions, based on a search of the CCSD.

A β-D-glucopyranosyl unit with a stable $^4C_1$ chair conformation bridges the two divalent metal ions with the μ-η^1:η^1-alkoxo group at C-2 position and the C-1 *N*-glycosidic amino and the C-3 hydroxyl groups coordinating to the terminal and central metal ions, respectively (Figure 8). The glucopyranosyl unit utilizes three sequential donor atoms on C-1, C-2, and C-3 positions that are arranged in a trans,trans configuration or an equatorial-equatorial-equatorial fashion. This arrangement is in contrast with the mannopyranosyl residue in complexes **4**, which join the Mn^{II} and Mn^{III} centers by using the cis,cis or equatorial−axial−equatorial donors on C-1, C-2, and C-3 positions (Figure 2).[7c] The C-2 μ-alkoxo bridge is symmetric with relatively short bond lengths to the terminal M ions of 1.97 (**31**) and 1.926 Å (**34**) and to the central M′ ions of 1.93 (**31**) and 1.932 Å (**34**). The average M−O_2−M′ angles are 123.7° (**31**) and 125.8° (**34**). The interaction between the central metal ions and the C-3 hydroxyl groups of the sugars are weak, and the M′−O_3 distances can be divided into two groups. There are longer distances of 2.66(1) (**31**) and 2.721(8) Å (**34**) and shorter ones of 2.39(1) (**31**) and 2.445(8) Å (**34**). The average N_1−M−O_2 and O_2−M′−O_3 bite angles are 82.6° (**31**), 86.5° (**34**) and 75.4° (**31**), and 74.5° (**34**), respectively. These two fused five-membered chelate rings might cause some strain in the six-membered pyranose ring. Unlike complex **4**, which involves almost linear $Mn^{II}Mn^{III}Mn^{II}$ trimetallic cores, the M···M′···M assemblies in **31** and **34** are bent, with angles of 155.18(8)° (**31**) and 161.56(6)° (**34**) formed by the carboxylate bridges of the XDK ligand. Notably, these compounds are the first examples of trimetallic systems stabilized by an XDK ligand. The other sugar moieties anchoring the terminal metal centers have very similar structures to those found in the mononuclear complexes **11** (M = Zn) and **12** (M = Cu). Their C-2 hydroxyl groups interact with the terminal metal ions weakly by comparison with the bridging sugar residues.

Table 6. Selected Bond Distances (Å) and Angles (Deg) for **31**·4.5MeOH·3.5H_2O[a]

bond distances			
Zn(1)−O(12)	1.966(9)	Zn(1)−O(22)	2.25(1)
Zn(1)−O(101)	1.99(1)	Zn(1)−N(11)	2.20(1)
Zn(1)−N(12)	2.19(1)	Zn(1)−N(13)	2.14(1)
Zn(2)−O(12)	1.95(1)	Zn(2)−O(13)	2.66(1)
Zn(2)−O(32)	1.91(1)	Zn(2)−O(33)	2.39(1)
Zn(2)−O(102)	2.06(1)	Zn(2)−O(202)	2.09(1)
Zn(3)−O(32)	1.97(1)	Zn(3)−O(42)	2.45(1)
Zn(3)−O(201)	2.00(1)	Zn(3)−N(21)	2.24(1)
Zn(3)−N(22)	2.15(1)	Zn(3)−N(23)	2.11(1)
bond angles			
O(12)−Zn(1)−O(22)	91.7(4)	O(12)−Zn(1)−O(101)	98.4(4)
O(12)−Zn(1)−N(11)	82.5(4)	O(12)−Zn(1)−N(12)	158.7(4)
O(12)−Zn(1)−N(13)	109.4(4)	O(22)−Zn(1)−O(101)	92.1(4)
O(22)−Zn(1)−N(11)	90.2(4)	O(22)−Zn(1)−N(12)	74.8(4)
O(22)−Zn(1)−N(13)	156.6(4)	O(101)−Zn(1)−N(11)	177.5(5)
O(101)−Zn(1)−N(12)	98.4(5)	O(101)−Zn(1)−N(13)	94.7(5)
N(11)−Zn(1)−N(12)	81.3(5)	N(11)−Zn(1)−N(13)	82.8(5)
N(12)−Zn(1)−N(13)	82.1(5)	O(12)−Zn(2)−O(13)	73.1(4)
O(12)−Zn(2)−O(32)	157.5(4)	O(12)−Zn(2)−O(33)	88.5(4)
O(12)−Zn(2)−O(102)	103.1(4)	O(12)−Zn(2)−O(202)	92.3(4)
O(13)−Zn(2)−O(32)	87.2(4)	O(13)−Zn(2)−O(33)	81.8(3)
O(13)−Zn(2)−O(102)	166.3(4)	O(13)−Zn(2)−O(202)	87.1(4)
O(32)−Zn(2)−O(33)	77.7(4)	O(32)−Zn(2)−O(102)	93.5(4)
O(32)−Zn(2)−O(202)	97.6(4)	O(33)−Zn(2)−O(102)	85.0(4)
O(33)−Zn(2)−O(202)	168.0(4)	O(102)−Zn(2)−O(202)	106.4(4)
O(32)−Zn(3)−O(42)	95.5(4)	O(32)−Zn(3)−O(201)	97.0(4)
O(32)−Zn(3)−N(21)	82.6(4)	O(32)−Zn(3)−N(22)	159.0(5)
O(32)−Zn(3)−N(23)	108.9(5)	O(42)−Zn(3)−O(201)	84.0(4)
O(42)−Zn(3)−N(21)	92.4(4)	O(42)−Zn(3)−N(22)	72.4(4)
O(42)−Zn(3)−N(23)	153.8(5)	O(201)−Zn(3)−N(21)	176.3(4)
O(201)−Zn(3)−N(22)	98.6(5)	O(201)−Zn(3)−N(23)	101.8(5)
N(21)−Zn(3)−N(22)	80.9(5)	N(21)−Zn(3)−N(23)	81.7(5)
N(22)−Zn(3)−N(23)	81.4(5)	Zn(1)−O(12)−Zn(2)	121.4(5)
Zn(2)−O(32)−Zn(3)	126.0(5)		

[a] Estimated standard deviations are given in parentheses.

EXAFS and NMR Spectroscopy. To elucidate the solution structure of complex **31**, Zn K edge X-ray absorption spectra were measured for powdered samples of **11** and **31** and for a solution sample of **31** (~0.1 M in DMF). Fourier transforms of the EXAFS data are shown in Figure 9. The spectrum of the powdered sample of **31** displayed three distinct peaks at about 1.6, 2.5, and 3.1 Å (before phase-shift correction), which were assigned to backscattering contributions of the nitrogen and

(27) Zhang, B.; Zhang, S.; Wang, K. *J. Chem. Soc., Dalton Trans.* **1996**, 3257.
(28) (a) Angyal, S. J. *Chem. Soc. Rev.* **1980**, *9*, 415. (b) Angyal, S. J. *Adv. Carbohydr. Chem. Biochem.* **1989**, *47*, 1.

Table 7. Selected Bond Distances (Å) and Angles (Deg) for **34**·3.5MeOH·2H_2O[a]

bond distances			
Zn(1)−O(12)	1.918(8)	Zn(1)−O(13)	2.445(8)
Zn(1)−O(32)	1.945(7)	Zn(1)−O(33)	2.721(8)
Zn(1)−O(102)	2.031(8)	Zn(1)−O(201)	2.031(8)
Cu(1)−O(12)	1.927(7)	Cu(1)−O(22)	2.626(9)
Cu(1)−O(101)	1.970(8)	Cu(1)−N(11)	2.10(1)
Cu(1)−N(12)	2.113(9)	Cu(1)−N(13)	2.23(1)
Cu(2)−O(32)	1.934(7)	Cu(2)−O(42)	2.421(8)
Cu(2)−O(202)	1.963(8)	Cu(2)−N(21)	2.069(9)
Cu(2)−N(22)	2.112(9)	Cu(2)−N(23)	2.21(1)

bond angles			
O(12)−Zn(1)−O(13)	77.2(3)	O(12)−Zn(1)−O(32)	153.1(3)
O(12)−Zn(1)−O(33)	85.0(3)	O(12)−Zn(1)−O(102)	96.7(3)
O(12)−Zn(1)−O(201)	97.1(3)	O(13)−Zn(1)−O(32)	86.2(3)
O(13)−Zn(1)−O(33)	82.4(3)	O(13)−Zn(1)−O(102)	167.1(3)
O(13)−Zn(1)−O(201)	83.7(3)	O(32)−Zn(1)−O(33)	71.8(3)
O(32)−Zn(1)−O(102)	95.0(3)	O(32)−Zn(1)−O(201)	102.1(3)
O(33)−Zn(1)−O(102)	85.7(3)	O(33)−Zn(1)−O(201)	165.2(3)
O(102)−Zn(1)−O(201)	108.5(3)	O(12)−Cu(1)−O(22)	97.5(3)
O(12)−Cu(1)−O(101)	94.6(3)	O(12)−Cu(1)−N(11)	86.8(3)
O(12)−Cu(1)−N(12)	165.7(4)	O(12)−Cu(1)−N(13)	107.8(3)
O(22)−Cu(1)−O(101)	80.3(3)	O(22)−Cu(1)−N(11)	95.1(3)
O(22)−Cu(1)−N(12)	73.2(3)	O(22)−Cu(1)−N(13)	154.4(3)
O(101)−Cu(1)−N(11)	175.4(4)	O(101)−Cu(1)−N(12)	94.4(3)
O(101)−Cu(1)−N(13)	101.2(3)	N(11)−Cu(1)−N(12)	83.4(4)
N(11)−Cu(1)−N(13)	82.5(4)	N(12)−Cu(1)−N(13)	81.2(4)
O(32)−Cu(2)−O(42)	92.2(3)	O(32)−Cu(2)−O(202)	96.0(3)
O(32)−Cu(2)−N(21)	86.2(3)	O(32)−Cu(2)−N(22)	163.9(3)
O(32)−Cu(2)−N(23)	109.6(3)	O(42)−Cu(2)−O(202)	89.3(3)
O(42)−Cu(2)−N(21)	89.8(3)	O(42)−Cu(2)−N(22)	74.8(3)
O(42)−Cu(2)−N(23)	156.6(3)	O(202)−Cu(2)−N(21)	177.6(3)
O(202)−Cu(2)−N(22)	93.4(3)	O(202)−Cu(2)−N(23)	96.4(4)
N(21)−Cu(2)−N(22)	84.3(4)	N(21)−Cu(2)−N(23)	83.6(4)
N(22)−Cu(2)−N(23)	82.2(4)	Zn(1)−O(12)−Cu(1)	128.3(4)
Zn(1)−O(32)−Cu(2)	123.3(4)		

[a] Estimated standard deviations are given in parentheses.

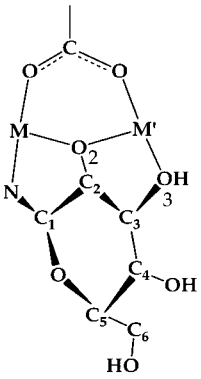

Figure 8. The MM′ bridging structure of complexes **31** and **34**.

oxygen atoms (N/O) coordinated to zinc, the carbon atoms (C) of the five-membered chelate rings, and the outer zinc atom (Zn), respectively, by Fourier filtered pre-curve-fitting analyses. In the spectrum of mononuclear **11**, no conspicuous peak was observed at 3.1 Å. The N and O atoms involved in the first coordination sphere could not be distinguished in the present analyses. The Fourier filtered (r = 1.1−3.5 Å) EXAFS data, $k^3\chi(k)_{obsd}$, were subjected to curve-fitting analyses with a three-wave model, $k^3\chi(k)_{calcd} = k^3\chi(k)_{N/O} + k^3\chi(k)_C + k^3\chi(k)_{Zn}$, and the structural parameters derived from EXAFS analyses are summarized in Table 8. The Zn···Zn separation determined by EXAFS of 3.49(4) Å is slightly longer than the average value of 3.440(4) Å determined by X-ray crystallography. The spectrum of the solution sample of **31** is very close to that of the powdered sample, strongly indicating that the trimetallic

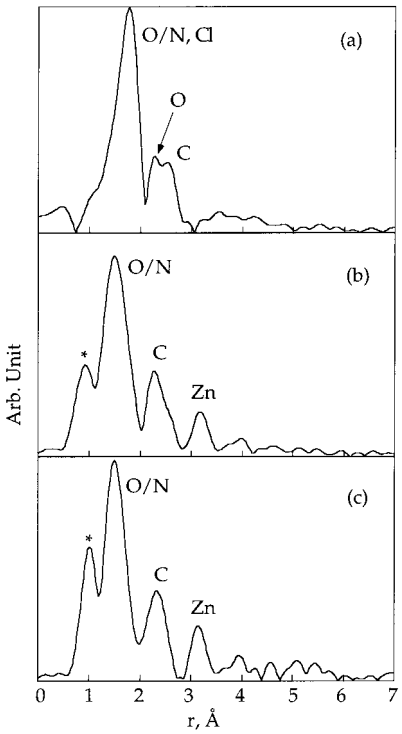

Figure 9. EXAFS Fourier transforms for (a) **11** (powder), (b) **31** (powder), and (c) **31** (solution).

structure determined by X-ray crystallography is retained in solution (Table 8).

Since **31** was not very soluble in methanol, complex **31***, having 1-^{13}C-enriched D-glucose, [1-^{13}C]-D-Glc, was prepared to measure a $^{13}C\{^1H\}$ NMR spectrum. The $^{13}C\{^1H\}$ spectrum of **31*** in the region of the C-1 anomeric carbons, shown in Figure 10, consists of two resonance sets around δ 94.8 and 97.5 ppm in a 1:1 ratio. The former is assignable to the C-1 carbons of D-glucopyranosyl moieties chelating to the terminal zinc ions by analogy with the chemical shifts observed for the mononuclear complex **11** (94.2 ∼ 94.9 ppm). The downfield shifted resonances at δ 97.4 and 97.6 would appear to correspond to the two inequivalent C-1 carbon atoms of the bridging D-glucopyranosyl units. The spectral pattern is consistent with the crystal structure, and clearly demonstrates that the bridging structure by the C-2 alkoxo group renders the C-1 anomeric carbon somewhat electron-deficient.

Conclusion

In the present study, the homo and heterotrimetallic zinc(II) and copper(II) complexes involving D-glucopyranosyl and biscarboxylate bridging ligands, $[M_2M'\{(D\text{-Glc})_2\text{-tacn}\}_2(XDK)]Cl_2$, were prepared by reactions of the sugar-binding mononuclear complexes, $[M\{(D\text{-Glc})_2\text{-tacn}\}Cl]Cl$ (M = Zn, Cu), with {M′(XDK)} fragments (M = Zn, Cu). The observed bridging system of β-glucopyranosyl with the C-2 μ-alkoxo group is the first structurally characterized example. The trinuclear complexes involve MM′ divalent dimetal centers bridged by a carboxylate group and a C-2 alkoxo group of D-glucopyranosyl moiety. They may be regarded as a model for substrate binding in glucose or xylose isomerases, in which aldose−ketose isomerization is promoted at dimetallic centers of Mg^{2+}, Mn^{2+}, and Co^{2+}. A bridging glutamate residue and an aldose in the open-chain form link the dimetal center, and the C-2 alkoxo bridge is activated toward 1,2-hydride shift, a key step leading to ketose.[2]

Table 8. Structural Parameters Derived from EXAFS Analyses

compound[a]	shell	A−B[a]	N[b,g]	r, Å[c]	σ, Å[d]	ΔE[e]	R, %[f]
[Zn{(D-Glc)$_2$-tacn}Cl]Cl (**11**, powder)	first	Zn−O/N	5.0	2.16	0.069	16.4	0.050
		Zn−Cl	1.1	2.31	0.130	−6.1	
	second	Zn−O	0.8	2.49	0.030	7.8	
		Zn−C	11.6	2.99	0.105	4.1	
[Zn$_3${(D-Glc)$_2$-tacn}$_2$(XDK)]Cl$_2$ (**31**, powder)	first	Zn−O/N	5.0[g]	2.02	0.104	5.7	0.065
	second	Zn−C	9.3[g]	2.94	0.105	0.3	
	third	Zn−Zn	1.3[g]	3.49	0.117	4.0	
[Zn$_3${(D-Glc)$_2$-tacn}$_2$(XDK)]Cl$_2$ (**31**, solution)	first	Zn−O/N	4.2	2.01	0.090	4.8	0.095
	second	Zn−C	9.1	2.93	0.093	−0.2	
	third	Zn−Zn	0.8	3.47	0.089	2.4	

[a] A is absorbing and B is backscattering atoms. [b] Coordination number. Estimated error is ±1. [c] Interatomic distance in Å. Estimated error is ±0.03 for the first shell and ±0.04 for the second and third shells. [d] Debye−Waller factor. [e] Shift of energy in eV from E_0. [f] $R = [\sum(\boldsymbol{k}^3\chi_o(\boldsymbol{k}) - \boldsymbol{k}^3\chi_c(\boldsymbol{k}))^2/\sum(\boldsymbol{k}^3\chi_o(\boldsymbol{k}))^2]^{1/2}$. $\chi_o(\boldsymbol{k})$ and $\chi_c(\boldsymbol{k})$ are Fourier-filtered (Δr =1.1 − 3.5 Å) and calculated data, respectively. $\boldsymbol{k}^3\chi_c(\boldsymbol{k}) = \boldsymbol{k}^3\chi_{O/N}(\boldsymbol{k}) + \boldsymbol{k}^3\chi_C(\boldsymbol{k}) + \boldsymbol{k}^3\chi_{Zn}(\boldsymbol{k})$ for complex **31** and $\boldsymbol{k}^3\chi_c(\boldsymbol{k}) = \boldsymbol{k}^3\chi_{O/N}(\boldsymbol{k}) + \boldsymbol{k}^3\chi_{Cl}(\boldsymbol{k}) + \boldsymbol{k}^3\chi_O(\boldsymbol{k}) + \boldsymbol{k}^3\chi_C(\boldsymbol{k})$ for complex **11**. [g] Coordination numbers are referenced to complex **31** (powder).

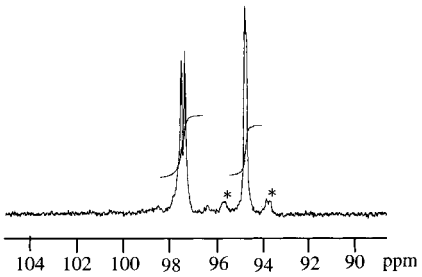

Figure 10. $^{13}C\{^1H\}$ NMR spectrum (the anomeric carbon region) of [Zn$_3${([1-^{13}C]-D-Glc)$_2$-tacn}$_2$(XDK)]Cl$_2$ (**31***) in CD$_3$OD.

Acknowledgment. We are grateful to Ms. Fujiko Yoshida for her helpful assistance in the preparation of the sugar complexes. This work was partially supported by a Grant-in-Aid for International Scientific Research (Joint Research) and a Grant-in-Aid for Scientific Research from the Ministry of Education, Science, Culture, and Sports, Japan, and by the U.S. National Science Foundation.

Supporting Information Available: Tabulations of crystallographic data, positional and thermal parameters, bond lengths and angles of non-hydrogen atoms for **11**·H$_2$O, **12**·MeOH, **13**·H$_2$O, **14**·H$_2$O, **15**·2MeOH, **22**·CH$_2$Cl$_2$, **31**·4.5MeOH·3.5H$_2$O, and **34**·3.5MeOH·2H$_2$O (61 pages); ORTEP plots of complexes **12**·MeOH, **13**·H$_2$O, and **14**·H$_2$O; X-ray absorption spectra, raw EXAFS data, and curve-fitting results for complexes **11** and **31**. These materials are available free of charge via the Internet at http://pubs.acs.org.

IC001419T